

PRNC-116

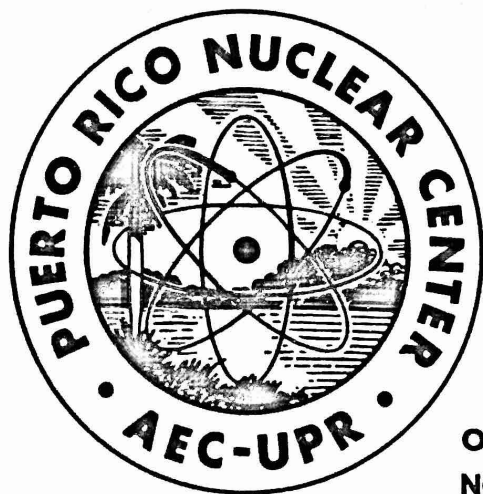
PUERTO RICO NUCLEAR CENTER

MATRIX ISOLATION STUDIES OF THE GAMMA-RADIOLYSIS
OF HETEROCYCLIC MOLECULES

Technical Progress Report #3

A. Grimison and G. A. Simpson

April 1968



OPERATED BY UNIVERSITY OF PUERTO RICO UNDER CONTRACT
NO. AT (40-1)-1833 FOR U. S. ATOMIC ENERGY COMMISSION

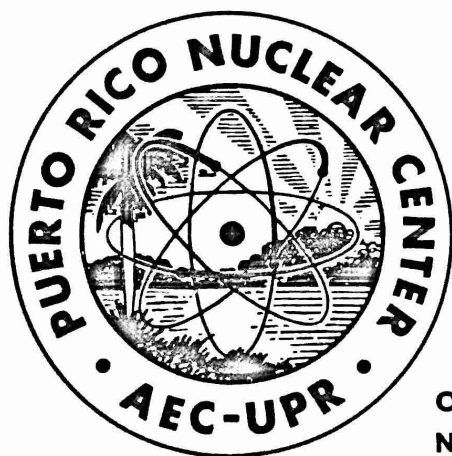
PUERTO RICO NUCLEAR CENTER

MATRIX ISOLATION STUDIES OF THE GAMMA-RADIOLYSIS OF HETEROCYCLIC MOLECULES

Technical Progress Report #3

A. Grimison and G. A. Simpson

April 1968



OPERATED BY UNIVERSITY OF PUERTO RICO UNDER CONTRACT
NO. AT (40-1)-1833 FOR U. S. ATOMIC ENERGY COMMISSION

Personnel Participating:

Dr. A. Grimison, Chief Scientist, Principal Investigator

Dr. G. A. Simpson, Associate Scientist

M. Trujillo, Graduate Student Assistant

S. Quadri, IAEA Participant

O. Pérez, Research Assistant (Part-time)

The results achieved in this project from May 1966 to April 1967 were previously presented in Technical Progress Reports No. 1 (PRNC Publication No. 88) and 2 (PRNC Publication No. 99). The present Technical Progress Report reviews the results obtained in the period from April 1967 to April 1968, the time of preparing this report. As done before, it is convenient to divide the work into two sections, Experimental and Theoretical.

I. Absorption Spectra of Radiolytic Intermediates at 77°K.

The general approach and techniques in this section of the work have remained the same as described in PRNC Publications No. 88 and 99. However, a series of absorption studies of intermediates produced in 3-methylpentane (3MP) have been initiated to parallel the emission studies reported in Part II of the Experimental Section (Table 1).

A specific attempt has been made to observe the radical anions of pyridine, pyrazine, pyridazine, and pyrimidine by radiolysis in 2-methyltetrahydrofuran (MTHF) glasses. This stems from our earlier observation (PRNC 99) of a high efficiency of electron scavenging for these azines and diazines. The spectra of species assigned to these radical anions have previously been reported by Hush et. al. ⁽¹⁾ In their work the neutral heterocyclic molecules were reduced by metallic sodium in MTHF at room temperature. The results from our radiolysis experiments are compared with those of Hush in Table 2. The general agreement is very good, suggesting that the radical anions are among the species formed on gamma-radiolysis. This appears to be the first case where the importance of ionic intermediates in the radiolysis of heterocyclic compounds has been established.

Considering the detailed comparison of the results for pyridine and the diazines, the agreement for pyridazine is excellent. The absorption at 354 nm in irradiated pyridazine in MTHF is observed to increase on bleaching the trapped electron band. This confirms the assignment of the 354 nm band to the pyridazine radical anion. For pyridine and pyrazine the slight variations observed from Hush's values have prompted us to undertake a detailed examination of these systems. Figure 1 shows the dependence of the absorption at 350 nm and 1200 nm in the irradiated pyridine-MTHF system of the initial pyridine concentration. The 1200 nm band corresponds to the position of the trapped electron band in MTHF. The figure clearly shows how the trapped electron absorption decreases with increasing pyridine concentration. Simultaneously the 350 nm absorption decreases, however, this is mainly accounted for by residual absorption of the 1200 nm band into the 350 nm region. This residual absorption also decreasing with the trapped electron concentration. It is observed that the 1200 nm band can never be completely scavenged by pyridine. A possible interpretation of this fact is that the anion has a band at 1200 nm, in addition to the 350 nm band. Two independent observations support this view. The first is obtained from experiments with photolysis (bleaching) into the 1200 nm band of gamma-irradiated pyridine-MTHF solutions. Since the 1200 nm band is mainly attributed to the trapped electron band in MTHF, photolysis in this band is expected to liberate electrons which can be captured by normal pyridine molecules, producing an increase in the concentration of the pyridine radical anion, and thus an increase in the 350 nm absorption. This is indeed observed in the concentration range below 4×10^{-2} M pyridine. However, at higher concentrations, bleaching

causes a decrease in the 350 nm absorption. This is compatible with an actual photolysis of the radical anion, occurring via its 1200 nm absorption, when this is appreciable relative to the trapped electron 1200 nm absorption. The second supporting observation stems from radiolysis experiments on pyridine in 3MP. In 3MP the trapped electron band occurs at 1800 nm, and in addition to this, bands at 360 nm and 1200 nm can be observed. Finally, the preliminary results of Pariser-Parr-Pople calculation for the pyridine anion reported later (Table 8) give the lowest energy transitions at 4.0 eV and 0.8 eV, in excellent agreement with the above assignment of 3.6 eV (350 nm) and 1 eV (1200 nm). The investigation of this system is continuing, and additional experiments have shown that the presence of water in the pyridine-MTHF system completely suppresses the formation of the 350 nm band.

The work on solutes in the glassy Freon matrix (FM) has continued. The preliminary note describing the characteristics of the matrix was appended to the previous Progress Report (PRNC 99). At the suggestion of the editors and reviewers of the Journal of Physical Chemistry, this note was extended to a full paper by the inclusion of our results on a number of heterocyclic molecules in FM, and is in press. A copy is appended to this report. The highlights include the characterization of cationic species formed by gamma-radiolysis of the FM matrix. The suitability of this matrix for stabilization of cationic intermediates is demonstrated by the detection of cationic species formed from several heterocyclic additives. In particular, the thiophene radical cation was assigned λ_{\max} at 830 and 320 nm, the pyrrole radical cation. λ_{\max} at 800 and 310 (?) nm, and the pyridine radical cation λ_{\max} at 380 nm. The results for pyrrole and pyridine are in excellent accord with the Pariser-Parr-Pople calculations reported later

(Tables 8 and 9). These gives pyrrole radical cation transitions at 1.2 and 3.8 eV as against the above assignment of 1.5 eV (800 nm) and possibly 4.1 eV (310 nm). The pyridine radical cation is calculated to have a transition at 3.2 eV, to be compared with the above assignment of 3.3 eV (380 nm).

The results obtained on gamma-radiolysis of indole in FM (Table 1) are surprising in comparison with the photochemical results (A, Part IV), and also the flash photolysis studies of Grossweiner.² The spectra suggest that if the 420 nm band reported in photolyzed indole is present, it may have been shifted by overlapping with the FM 585 nm band. Closely spaced maxima are observed in the region from 450 to 700 nm, and a strong band at 1100 nm. The latter band may be associated with the 420 nm band, assigned to the indole radical cation, which is likely product of the FM radiolysis. However, the 1100 nm band could not be detected in the steady state or flash photolyses experiments. The complex maxima in the 450 to 700 nm region suggest the presence of at least one other species. Optical bleaching experiments and 3MP radiolysis are being made on indole to clarify these points.

II. Luminescence of Irradiated Glassy Solutions at 77°K

The purpose of the luminescence experiments is two-fold. The first is to determine whether gamma-irradiation produces species having different emission spectra when excited by ultraviolet light of a suitable wavelength. The second is to search for recombination luminescence by infrared or thermal excitation of the system subsequent to gamma-irradiation. A radiation

induced luminescence has been observed in irradiated 3 MP,³ and is considered to result from excitation of a charge separated state of the aliphatic hydrocarbon. Hamill⁴ has reported recombination luminescence of a large number of aromatic solutes in 3MP, stimulated by either infrared or thermal excitation of the matrix. He attributes this luminescence to the result of either electron-cation or cation-anion recombination in the matrix, depending upon solvent rigidity.

Luminescence studies have been limited almost exclusively to 3MP after a test on the ability of TMPD to undergo thermally stimulated emission in either MTHF or FM irradiated matrices. Hamill maintains (private communication) that the absence of an effect may be expected in MTHF since only anionic additives are stabilized. A recombination event between that anion and a solvent cation would result in the excitation and decomposition of the solvent. In FM the TMPD is observed to form a colored, salt-like product on warming. Possibly recombination in this matrix involves bond formation between the cationic additive and a halide ion.

The results of the investigations into these effects are reported in Table 3 and Fig. 2. The luminescence spectra were obtained with an Aminco Bowman Spectrophotofluorometer using either the Aminco low temperature optical dewar for small 1/8" od silica tubes, or a square quartz dewar for larger 1 x 1 cm square optical cells. The larger cells provide greater intensity of luminescence than the smaller tubes, although their use presents some problems in detection of new emission bands. The square quartz dewar itself emits a number of bands on excitation with light near 250 nm with λ_{max} at 300, 400 and 555 nm. Thus, this dewar is used only for determining emission bands resulting from thermal excitation. Infrared stimulation has not been attempted so far.

Figure 2 provides a demonstration of the thermal excitation experiment which is similar in principle to experiments which determine "glow curves". The cell in the dewar is allowed to warm up by removing the liquid nitrogen from the dewar and monitoring the emissions by repeatedly scanning with the spectrometer. Thus, the time dependence of the emission spectra is obtained. The results for the luminescence of pure 3MP are in good agreement with those of the Funabashi group.³ Immediately after warming, luminescence near 425 nm is produced. At higher temperatures this shifts to shorter wavelengths, due to an emission resulting from radiation-induced olefin production. When other compounds are dissolved in 3MP, the 3MP emission band is reduced in intensity and emission bands associated with the additive are produced. These effects have been observed for the following compounds; biphenyl, DNA, pyridine, pyrazine, pyrrole, naphthalene (MTHF solvent), thiophene, toluene, and triphenylamine. The results with biphenyl and triphenylamine have been reported earlier by Hamill and Skelly.⁴ Emissions from γ -irradiated toluene on warming have been observed previously by Brocklehurst et. al.,⁵ and from photolyzed toluene on u.v. excitation by Porter.⁶ The similarity of the thermoluminescence emission bands of toluene following γ -irradiation to those induced by u.v. excitation suggest that excitation of neutral benzyl radicals is also being produced in the thermoluminescence study.

Some results which were obtained with irradiated silica tubes (suprasil) are of considerable interest. An absorption band with λ_{max} at 256 nm is produced on irradiation, and this band disappears on warming. Excitation into this band was observed to produce an emission at 310 nm. These effects are assigned to hydroxyl radicals arising from water adsorbed on the surface of the silica for a number of reasons. Water is strongly absorbed on silica, and it is known that hydrogen atoms are produced by radiolysis of this water,⁷ with an enhanced yield.⁸ The presence of hydroxyl radicals is therefore indicated, although they have not been previously identified in this system. Hydroxyl radicals are known to absorb in the 250 nm region of the spectrum, and have λ_{max} at 260 nm⁹ in aqueous solutions. The hydroxyl radical exhibits an emission band at 306 nm in the gas phase.¹⁰

A warm-up glow from irradiated solutions of pyridine in 3MP occurring at 330 nm has been observed, persisting for long times (10 to 20 minutes) after removal of the liquid nitrogen. The absorption spectrum has for this solution λ_{max} at 360 and 1200 nm. The 1200 nm band has been assigned to the pyridine anion (earlier), together with a band at 350 nm. The cation shows a λ_{max} at 380 nm (attached preprint). The spectrum in 3MP might therefore be due to the superposition of the radical anion and radical cation spectra, the bands at 350 and 380 nm not being resolved. The long lived luminescence observed can therefore be tentatively assigned to the recombination of cations and anions. This is expected to be a diffusion-controlled reaction, but the low rate is compatible with the high viscosity of the glass at these low temperatures, even after some softening has occurred.

A test can be made by a comparison of the temperature dependence of the absorption spectra and that of the emission spectra. A slight raise in temperature would be expected to liberate some of the trapped electrons to recombine with neutral pyridine molecules and pyridine cations to yield a low temperature luminescence, and a shift in the absorption maximum from 360 to 350 nm. At higher temperatures, the decrease in the absorption bands and in the long-lived luminescence should follow the same kinetics.

The phosphorescence from the triplet state of pyridine has been reported at 370 nm.¹¹ This difference in wavelength is somewhat outside the limit of experimental error. Nevertheless as a preliminary hypothesis the emitting species can be taken as the triplet state of pyridine until an exact comparison of the pyridine phosphorescence and the thermoluminescence can be made.

III. Electron Spin Resonance of Radiolytic Intermediates at 77°K

The principal work on electron spin resonance has been related to intermediates in the irradiated freon mixture (FM). Figure 3 shows some of the ESR spectra of irradiated FM obtained on a Varian E-3 ESR spectrometer at the Chemistry Department, University of Puerto Rico. The resonance associated with the degassed, irradiated sample and tube is very complex, extending over 500 gauss (spectrum 3a), and containing unresolved structure. The analysis is further complicated by the hydrogen atom⁷ and other resonances, which undergo changes on exposure to visible light. This suggests, that, in addition to hydrogen atoms and the hydroxyl radicals proposed in this report, another species absorbing in the visible region, such as the trapped electron or absorbed H_2O^- may be present. (See Figure 3 b)

Due to these factors, attempts were made to irradiate and take the ESR spectra of frozen FM droplets in liquid nitrogen. Unlike the absorption spectra, the ESR spectra are found to be strongly influenced by the presence of oxygen. Spectrum 3c was obtained by dropping aerated FM into liquid nitrogen, and spectrum 3d by extruding glassy, degassed FM into liquid nitrogen. The lack of detailed structure in 3d compared to 3a indicates that some air contamination of FM has occurred despite precautions.

Bleaching experiments indicated that the principal effect of the ESR spectrum of photolyzing irradiate FM with visible light (see attached preprint for effects on the absorption spectrum) is to increase the resonances in the center portion of the spectrum, near $g = 2$. This can be correlated with the increase in the absorption of irradiated FM at wavelengths less than 300 nm on bleaching. The only ESR signals which decrease on bleaching are the extreme left to the spectrum (field approx. 2800 gauss and frequency 9.2 gigacycles/sec). These signals can therefore be correlated with the positively charged species in irradiated FM with absorptions bands near 330 and 585 nm, which are removed by bleaching.

IV. Photochemistry of Aromatic Amines and Heterocyclic Compounds at 77°K

Recent evidence has demonstrated the generality of the biphotonic ionization of a large class of compounds,⁶ via their triplet states. It is conceivable that radical cations of heterocyclic compounds can be generated in this fashion. Since neutral radicals can also be produced via simple excitation transfer, photolysis provides an independent method of establishing the nature of radiation induced intermediates.

Photolysis were carried out in 1 cm square quartz cells in a square optical dewar with liquid nitrogen by exposing the dewar to the full arc

of a Mineralight R-51 low pressure mercury lamp, or an Osram HBO 500 high pressure mercury lamp. In order to test a theory of Hamill¹² on the effect of solvation in a polar solvent, and the effect of trapping a photoejected electron by a halogenated compound, all photolysis were repeated in Freon mixture (FM), 2-methyltetrahydrofuran (MTHF) and 3-methylpentane (3MP). Measurements of spectra of photolyzed, degassed samples at 77°K were made in a Bausch and Lomb 505 Recording Spectrophotometer. Table 4 shows the results obtained for photoionization of aromatic amines in comparison with previous work. Three points arise from this table. The first is that the intensities employed are sufficiently high to produce appreciable photoionization. The results are in excellent accord with those of earlier workers, except for the failure to produce photoionization of diphenylamine. The results for diethylaniline and ethylaniline obtained here are the first reports of steady state, as opposed to flash photolysis, photoionization of these compounds. The hypothesis of Hamill¹² is borne out by the results, since there is an enhancement of color formation in general in MTHF compared to 3MP.

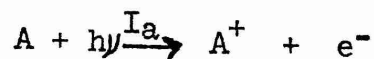
A large number of heterocyclic compounds were first screened visually for photoionization, and then the absorption spectra determined in favorable cases. The results are summarized in Tables 5 and 6. Of the compounds screened in this manner, only one previously reported to photolyze gave negative results. Douzou¹³ et. al. report a photoinduced absorption band of purine in aqueous solutions between 300 and 350 nm, together with ESR evidence for the solvated electron. The failure to observe similar results here is due to the fact that only visual observations were made.

The result with indole may be compared with the experiment of Grossweiner² in which indole was flash-photolyzed to yield the solvated

electron and band near 450 nm. However, in an earlier report¹⁴ by the same author there was evidence for several bands in the range 400 to 600 nm in addition to the band near 450, which was assigned to a neutral radical at that time rather than the indole radical cation. The λ_{\max} observed here is at 420 nm. The difference may be due to solvent shifts, although there appears to be a discrepancy between the two Grossweiner papers, since the earlier paper reports the indole band at 439 nm. This is one case where a direct comparison with the radiolysis work is being made (Part I).

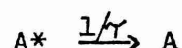
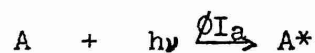
The absorption band produced at 370-400 nm on photolysis of Freon 114B2 can be compared with the species produced by Hamill and Bertin¹⁵ by γ -irradiation of methylbromide or sec. butylbromide in 3MP, and having λ_{\max} at 360 nm. A band having a similar bleaching response has also been observed in the γ -irradiation of alkyl iodides in 3MP.¹⁶ These bands have been assigned to the charge-transfer complex X.RX, arising from recombination of X^- and RX^+ . The photolyzed Freon 114B2 gives a bromine like color on warming, but the spectrum does not correspond to atomic bromine. By analogy with Hamill's work, this absorption may arise from a charge transfer complex between Br and FM or F114B2.

The fact that only 15 out of the 50 compounds tested gave colored intermediates on photolysis suggest that photoionization is generally an inefficient process in heterocyclic molecules. Let us consider the photoionization process in more detail. The direct photoionization of a neutral molecule A



is unexpected under these experimental conditions since the gas phase ionization potentials may be greater than 8 eV.¹⁷ Photoionization can be

produced by the biphotonic path



where A^* is a long lived excited state (probably a triplet), ϕ is the quantum yield for its formation, I_a is the intensity of light absorbed by A , γ is the lifetime of A^* , I_a' is the intensity of light absorbed by A^* , ϕ^+ the quantum yields for formation of e^- and A^+ . If ϵ , ϵ^* , c , c^* , d and d^* are the respective extinction coefficients, concentrations, and optical paths for A and A^* , we have that

$$I_a = I_0 \sqrt{1 - \text{Exp}(-\epsilon c d)}$$

$$\text{and } I_a' = I_0 \sqrt{1 - \text{Exp}(-\epsilon^* c^* d^*)}$$

In this case the exciting and ionizing photons are assumed to have the same energy, but similar arguments can be made for different photon energies. The primary energy requirement is now that $h\nu \leq (\text{I.P.} - E^*)$ where I.P. is the condensed phase ionization potential, and E^* the 0-0 energy of the excited states. Applying the steady state approximation and the (easily met) condition that the concentration of A is so large that the term $\exp(-\epsilon c d) = 0$ gives the rate of formation of A^+ as

$$d[A^+] / dt = \text{function of } (I_0^2 \phi \phi^+ \epsilon^* \tau / \epsilon c)$$

A computer program has been prepared which carries out this calculation for various values of the input parameters. Using the data of Meyer and Albrecht¹⁸ for the photoionization of N,N,N',N' Tetramethyl-p-phenylenediamine (TMFD) gave good results. Thus, a rationale is provided for the interpretation of

the results. The low efficiency of photoionization of the heterocyclic molecules tested may be due to insufficient photon energy, or insufficient light intensity. It would also be the result of a low quantum yield for formation, a short-triplet lifetime, or a low triplet extinction coefficient. These factors cannot be assessed completely at present. However, it is known that the triplet (n, π^*) lifetimes of some N-heterocyclics are shorter than those of the triplet (π, π^*) states of corresponding homocyclic compounds by factors of 1/1000.¹⁹

On the basis of the results, it is planned to modify the experimental procedure to permit (i) longer irradiation times (ii) use of a higher intensity lamp and (iii) use of as low a wavelength as feasible.

Section B.- Theoretical Work

The theoretical work has continued along the basic lines indicated in the previous Progress Report. As before, it is convenient to separate the results, according to the formalism used, into Molecular Orbital and Valence Bond calculations.

I. Molecular Orbital (M.O.) Calculations

The calculations currently being carried out utilize the Pariser-Parr-Pople (PPP) self-consistent field method²⁰ to calculate neutral molecule and radical spectra. The major defect of this method in the past has been the lack of justification for its use of repulsion integrals considerably (20%) lower than the theoretical values. However, recent non-empirical calculations on the excited states of the ethylene molecule²¹ have given this sorely-needed justification. These calculations show that the reduction in the repulsion integrals between pi-electrons is necessary to account for

the reorganization of the sigma-electron framework that occurs of excitation of a pi-electron.

The technique used here, in the spirit of the original Pariser-Parr method, is to search for the set of reasonable parameter values which give the best accord with the experimental singlet-singlet and singlet-triplet excitation energies of the neutral heterocyclic molecule. The same parameter values are then carried over unchanged to the calculation of the doublet-doublet excitation energies of the radical anion and radical cation of the same molecule. Such parameter searching is extremely time-consuming, but the initial results appear to justify this approach. The earlier computer program to carry out the PPP calculations on an IBM 1130 computer has been considerably refined, and a version now exists for the IBM 360 which will permit calculations on more complicated molecules. In particular, the PPP program is now linked on demand directly to a Configuration Interaction (CI) program described below.

The first molecule which has been carried through the full optimization procedure is pyrrole. These results were obtained after about 20 calculations, and supersede those reported in PRNC 99. The optimized parameters and the results obtained for pyrrole, pyrrole radical cation and pyrrole radical anion are compared with the experimental results in Table 7. The agreement between the theoretical transitions of the radical cation and the experimental values assigned earlier in this report is extremely good. The actual classification of the doublet transitions and the calculation of the doublet transition energies is discussed later.

The results obtained to date for pyridine and its radical anion and cation are reported in Table 8. Calculations have been made on pyridine and the pyridine radical anion previously by Hopton and Hush.¹ For comparison, their results are also shown in the Table. The calculations made by Hopton

and Hush differ in several important aspects from those reported here. Thus input Huckel wavefunctions for benzene were used, instead of the Huckel wavefunctions for pyridine used in the present work. A simplification was made by Hopton and Hush to the elements of the Hamiltonian Matrix which partly ignores the effect of electronic polarization. This simplification has not been made here. Finally, no attempt was made by Hopton and Hush to optimize the parameters used. The results in the table indicate that we obtain significantly better agreement between the theoretical and experimental transitions of pyrdine. More importantly, a very much better accord is obtained for the pyridine radical anion spectrum, as measured by Hopton and Hush. The results obtained for the pyridine radical cation are also in excellent accord with the assignment made earlier in the experimental section. A similar improved accord is found between our calculations and the experimental transition energies of the pyrimidine radical anion (Table 9).

Table 10 lists the results of a calculation made on the cyclopentadiene molecule, for comparison with the valence-bond calculation. The results are in excellent accord with the experimental singlet and triplet transitions.

The effect on the calculated singlet-singlet, singlet-triplet, and doublet-doublet excitations of introducing a limited amount of configuration interaction is now being studied. For the singlet and triplet states, configuration interaction is included among the excited configurations $m \rightarrow m+1$, $m \rightarrow m+2$, $m-1 \rightarrow m+1$, and $m-1 \rightarrow m+2$, where m is the highest doubly occupied orbital. No interaction terms arise between singlet and triplet excited configurations. The expressions for the singlet and triplet configuration interaction matrix elements are:-

Diagonal Elements (Since the ground state energy is subtracted from each for convenience, these correspond to the excitation energies to the various states).

$$[S(i \rightarrow j)/H/S(i \rightarrow j)] = e_j - e_i + 2(ij/ij) - (ii/jj)$$

$$[T(i \rightarrow j)/H/T(i \rightarrow j)] = e_j - e_i - (ii/jj)$$

where e_j and e_i are the calculated eigenvalues, and (ij/ij) and (ii/jj) are molecular repulsion integrals in the customary notation, that is,

$$(ij/ij) \equiv (u_i(1)u_i(2)/\frac{e^2}{r_{12}} / u_j(1)u_j(2))$$

$$\text{and } (ii/jj) \equiv (u_i(1)u_j(2)/\frac{e^2}{r_{12}} / u_i(1)u_j(2))$$

for molecular orbitals u_k . Since the molecular orbitals are expressed here as linear combinations of atomic orbitals, the molecular repulsion integrals are given as a linear combination of the atomic repulsion integrals used as input to the PPP program.

Off-diagonal Elements

$$[S(i \rightarrow j)/H/S(k \rightarrow l)] = 2(ij/kl) - (ik/jl)$$

$$[T(i \rightarrow j)/H/T(k \rightarrow l)] = -(ik/jl)$$

These expressions are identical to those given by Pople.²²

For the CI matrix of the doublet states, the ground and excited states were represented by the determinantal functions:-

$$(2_G) = \det(u_1 \bar{u}_i \dots u_1 \bar{u}_i u_m) \quad i = m-1$$

where the bar denotes beta spin, and m is the highest (singly) occupied level.

$$({}^2A) = \det(u_i \bar{u}_i \dots u_i \bar{u}_m u_m) \quad i \text{ to } m$$

$$({}^2B) = \det(u_i \bar{u}_i \dots u_i \bar{u}_k u_k) \quad m \text{ to } k (=m+1)$$

$$({}^2A') = \det(u_i \bar{u}_i \dots u_n u_i \bar{u}_i u_m) \quad h(=m-2) \text{ to } m$$

$$({}^2B') = \det(u_i \bar{u}_i \dots u_i \bar{u}_l u_l) \quad m \text{ to } l (=m+2)$$

$$({}^2C) = (2^{-1/2}) \left[\det(u_i \bar{u}_i \dots u_i u_k u_m) + \det(u_i \bar{u}_i \dots u_k \bar{u}_i u_m) \right] \quad i \text{ to } k$$

use of the approximation of Longuet-Higgins and Pople²³ gives rise to the following matrix elements: -

Diagonal

$$(A/H/A) - (G/H/G) = e_m - e_i + 0.5 (mm/mm) + 0.5 (im/im) - (ii/mm)$$

$$(A'/H/A') - (G/H/G) = e_m - e_h + 0.5 (mm/mm) + 0.5 (hm/hm) - (hh/mm)$$

$$(B/H/B) - (G/H/G) = e_k - e_m + 0.5 (mm/mm) + 0.5 (mk/mk) - (mm/kk)$$

$$(B'/H/B') - (G/H/G) = e_l - e_m + 0.5 (mm/mm) + 0.5 (ml/ml) - (mm/ll)$$

$$(C/H/C) - (G/H/G) = e_k - e_i + 2(ik/ik) - (ii/kk)$$

Off-diagonal

$$(A/H/G) = 0.5 (im/mm)$$

$$(A'/H/G) = 0.5 (hm/mm)$$

$$(B/H/G) = 0.5 (km/mm)$$

$$(B'/H/G) = 0.5 (lm/mm)$$

$$(C/H/G) = 0.0$$

$$(A'/H/A) = 0.5 (hm/im) - (hi/mm)$$

$$(B/H/A) = (im/mk)$$

$$(B'/H/A) = (im/ml)$$

$$(C/H/A) = (2^{-1/2}) \left[(ik/im) + 0.25 (mm/mk) - 0.5 (ii/mk) \right]$$

$$(B/H/A') = (hm/mk)$$

$$(B'/H/A') = (hm/ml)$$

$$(C/H/A') = (2^{-1/2}) \left[(ik/hm) - 0.5 (hi/mk) \right]$$

$$(B'/H/B) = 0.5 (mk/ml) - (mm/k1)$$

$$(C/H/B) = (2^{-1/2}) \left[(ik/mk) + 0.25 (mm/mi) - 0.5 (im/kk) \right]$$

$$(C/H/B') = (2^{-1/2}) \left[(ik/lm) - 0.5 (im/lk) \right]$$

A computer program has been written to generate the singlet and triplet configuration interaction or the doublet CI matrices. The matrices are diagonalized by a standard sub-routine to give the final excitation energies. This program links directly to use the output from the PPP program. It has been tested, and appears to work satisfactorily. This PPP-CI combination will now be employed on calculations on the diazines and their radical ions. After use on pyrrole and pyridine and their radical ions, this PPP-CI will be employed in calculations on the diazines and their radical ions.

III. Valence Bond (V.B.) Calculations

These calculations use the non-empirical VB method²⁴ to calculate the unpaired spin states of simple heterocyclic ring systems. Initially the triplet states of cyclopentadiene and the doublet states of the cyclopentadiene radical cation are being investigated. One great advantage of the valence-bond formalism for radical calculations does not appear to have been fully exploited in the past. This is that once the necessary formalism and integrals have been derived for the parent molecule, the radical cation calculation is carried out with no additional labor by equating all integrals involving the 'missing' electron to zero.

i) Formalism

All the possible 'structures' for the four-electron singlet, triplet, and quintuplet states were included; non-polar, polar and dipolar. These 'structures' were then expressed as a linear combination of singlet determinantal basis functions A_j . Since each basis function A_j is a linear combination of atomic orbitals a_i , integrals of the basis functions over the one- and two-electron operators ($A_j F A_k$) can be expressed as a linear combination of atomic integrals ($a_i F a_m$). For cyclobutadiene there are 2 non-polar, 12 polar, and 6 dipolar singlet structures, formed from combinations of 36 determinantal basis functions. There are also 3 non-polar, and 12 polar triplet structures, and 1 non-polar quintuplet state. Thus without the use of symmetry, the singlet energy levels form a 20 x 20 matrix, the triplet levels a 15 x 15 matrix, and the quintuplet state a one-element 'matrix'. However, by the use of group theory, the 'structures' can be grouped into combinations corresponding to the irreducible representations of the C_{2v} group, to which cyclopentadiene belongs. This gives a 12 x 12 matrix for the singlet A states, an 8 x 8 matrix for the singlet B_1 states, an 8 x 8 matrix for the triplet A_1 states, and a 7 x 7 matrix for the triplet B_1 states. As stated in PRNC 99, the formalism for obtaining these matrix elements from the basis integrals ($A_j F A_k$) has been completed. It is not reproduced here, as it is voluminous.

ii) Atomic Integrals

The next step is the calculation of the atomic integrals ($a_i F a_j$), where F is a one-electronic or bielectronic operator, or the identity operator. The integrals required in the particular formalism used are overlap

integrals (i/j), repulsion integrals (ii/jj) and (ij/ij), kinetic energy integrals (i/T/j), and core-attraction integrals (iiV⁺j) and (ijV⁺j). All of these integrals were calculated using Slater orbitals with a net of values from k = 1.0 to 2.0 in steps of 0.2, during two months spent by the principal investigator at the Theoretical Chemistry Center, University of Bologna. In particular, two different formulations were used for the potential due to an sp² hybridized C⁺ ion.

The Geoppert-Mayer-Sklar approximation for the latter potential gives $V^+(sp^2) = V^o(sp^3) - (\pi\pi/pp)$ where V^o represents the potential obtained by adding an electron to the 2p orbital of the C⁺ ion, and $(\pi\pi/pp)$ is the repulsion between this electron and an electron in the pi-framework of the molecule. The first method used is the usual one of assuming the electron added to a 2p orbital of a C atom, rather than a C⁺ ion, and thus using Slater orbitals throughout. The second method used here has been to employ an atomic potential derived from the self-consistent charge distributions given by Campadelli and Zauli.²⁵ The potential obtained (given incorrectly in PRNC 99) is

$$V^o(sp^3) = (R^{-1})(\text{Exp}(-11.25R) \sqrt{2} + 10.128R) \\ + \text{Exp}(-2.388R) \sqrt{4} + 7.80R).$$

From this potential, the form of the orbital p to be used in calculating the repulsion integral is also obtained. The appropriate integrals were calculated using the bicentric potential obtained from the Poisson equation as a linear combination of associated Legendre functions, as indicated by Tauber.²⁶

The values of the atomic integrals calculated for the four different atomic separations needed in the cyclopentadiene calculation, and the

previously mentioned parameter net, are listed in Tables 11-16. The values obtained agree very well with those reported previously for a few parameter values.²⁷ However, the present compilation is much more extensive, and the values of the integrals are calculated to a much greater precision.²⁸ There is a significant difference between the Slater and Self-consistent field approximations for the core attraction integrals in the expected direction, that is, a larger value for the SCF integrals.

iii) Basis Function Integrals

With the integrals among atomic orbitals evaluated, the integrals (A_iFA_j) among determinantal basis functions A_k can be calculated. This is rather tedious in sophisticated calculations, since the basis set is not assumed to be orthogonal, a serious defect of earlier work.²⁹ A computer program has been written and tested by Palmieri³⁰ which computes all the possible integrals (A_iFA_j) over mono- and bielectronic operators, given as input the atomic integrals. This program is being used to compute a set of (A_iFA_j) from each set of atomic integrals (one exponent value, one approximation for V^+) described above.

iv) 'Structure' Integrals

The next step consists of deriving the values for the Hamiltonian and overlap matrix elements by substitution of the basis function integrals into the expressions derived in part (i). The whole process of generating the 12×12 and 8×8 A_1 matrices, the 8×8 and 7×7 B_1 matrices, and then solving the matrix equations $[\bar{H}] - [\bar{E}][\bar{S}] = 0$ for the energy levels must be repeated for each set of atomic integrals, or twelve times in all. A computer program is therefore being written to carry out this procedure,

using as input the (A_1FA_j) values obtained from the Palmieri program. The first part of this program, to obtain the A_1 states, is almost complete.

TABLE 1.

New Absorption Maxima from Gamma-Irradiated Heterocyclic Molecules in Rigid Glasses at 77°K

Substance	Glass	Abs. Max. (nm)	Effect of bleaching solvent band
	Silica cell	254	increase (UV bleach)
Indole	Freon	1000, 620, 600, 565, 550	---
Imidazole	Freon	580	decrease
Pyrazole	MTHF	321	---
Pyrazole	3MP	360, 1200	---
Pyrrole	MTHF	below 400	decrease
Thiazole	MTHF	330	increase
Thiophene	MTHF	370, 670	increase
Thiophene	3MP	340, 830	decrease

TABLE 2.

Absorption Maxima of Gamma-Irradiated Pyridine, Pyridazine, and Pyrazine in MTHF Compared with Authentic Radical Anion Spectra (Hush and Hopton)

Parent Substance	Principal Absorption Maxima (nm)	
	Gamma-irradiation	Radical Anion
Pyridine	350	335
Pyridazine	354	351
Pyrazine	340	364

TABLE 3

Luminescence maxima* (nm) of irradiated heterocyclic or aromatic compounds at 77°K

Compound	Glass	Luminescence max before irradiation	Excitation	Warm up emission max
Silica tube	3MP	---	230	450 415***
Biphenyl	3MP	390, 415	300	500, 530, 570
DNA	3MP	450	290	450
Pyridine	3MP	--	--	330
Pyrazine	3MP	380, 405	300	375, 400
Pyrrole	3MP	425	276	None
Naphthalene	MTHF	425, 485, 590	300	500, 530, 570
Thiophene	3MP	460	290	550
Toluene**	3MP	300fl. 400 phos.	280	530
Thymine	3MP	400, 425	270	None
Triphenylamine	3MP	425	330	440

* λ Max are reproducible to ± 25 nm due to positioning in A-B spectrometer.

** emissions produced by uv photolysis also.

*** After gamma-irradiation, excitation at 230 nm produces a new emission at 310 nm.

TABLE 4

Photolysis of Aromatic Amines Using an Osram HBO500 Lamp at 77°K
Visual Observations or λ_{max} (nm)

Solute	Freon	MTHF	3 MeP	Reference
Aniline	Colorless	Pale yellow (406)	Tan yellow	(429) Proc. Roy. Soc. A230, 399 (1959)
Diethylaniline	Colorless	Tan-yellow	Colorless	-----
Dimethylaniline	Yellow-green	Faint yellow-green	Faint yellow-green	(459) J. Am. Chem. Soc. 65, 2424 (1943)
N,N-Dimethyl-p-phenylenediamine	Red* (525, 571)	Red* (529, 577)	Faint red* (530, 576)	(525, 575) J. Am. Chem. Soc. 86, 1297 (1964)
Diphenylamine	Light green (670)	Yellow-green	Light yellow-green	(680) J. Am. Chem. Soc. 64, 2801 (1942)
Diphenylmethylaniline	Colorless	Colorless	Colorless	(650) " " " " " "
Ethylaniline	Pale yellow	Strong yellow 410, 450)	---	-----
N,N,N',N'-Tetramethylbenzidine	Strong-yellow green	Strong yellow-green (360, 390, 440, 447, 550**)	Strong yellow green	(540, 790, 885) J. Am. Chem. Soc. 64, 2801 (1942)
Triphenylamine	Brown-pink (480-640)	Yellow green	Colorless	(656) J. Am. Chem. Soc. 86 (1964)

*Intense color resulted after 2 minutes exposure to lamp; all others required up to 30 minutes exposure.

**Spectra beyond 650 m μ not examined. Visual color and existence of one band near 550 suggest similarity of these absorptions.

TABLE 5

Compounds for which either no visual color was produced at 77°K after 30 min. exposure to full arc of either mineralight R-51 low pressure H_g lamp or HBO 500 Osram high pressure H_g lamp, or which exhibited no color formation after purification in either MTHF, 3MP, or Freon. (Concentrations of the order 10⁻² M or less, aerated solutions).

Adenine
 Aloxan
 Barbituric acid
 Benzimidazole
 Furan
 Hypoxanthine
 Hematophorphyrin
 Imidazole
 Isoxazole
 Methyltetrahydrofuran (an impurity resulting from an oxidation of MTHF forms a blue colored intermediate)
 N-methylhexylmorphine
 N-cyclohexylpiperidine
 N-methylpyrrole (contains an impurity which undergoes a photolytic reaction with Freon-II to produce a yellow intermediate which subsequently forms a green precipitate after warming.
 N-vinylpyrrolidine
 Pyrrole (see N-methylpyrrole)
 Pyrolidone
 Purine
 Pyrazine
 Pyrazole
 Quinoxaline (impurity forms yellow brown-intermediate which turns pink on warming)
 Thiophene
 Thiazole
 s-Triazine (yellow color on warming)
 Thymine

TABLE 6

Compounds producing a visual colored intermediate after photolysis at 77°K with up to 30 minutes exposure to either low (mineralight R-51) or high (OSRAM HBO-500) pressure lamps λ_{\max} reported in μ .

<u>Compound</u>	<u>Matrix</u>	<u>Color</u>
Chloroindole	3MP + F-11	Yellow
"	MTHF	Red-orange
Freon 114B2	Freon	Yellow (λ_{\max} 370-400), red brown color on warming
"	3MP	Yellow (λ_{\max} 370-400)
Dicyclohexylthiourea	Freon	Yellow*
Indazole	MTHF	Yellow-brown
"	3MP + F-11	sl-Yellow*
Indole	Freon	Yellow orange (λ_{\max} 390, 420, strong and 480) yellow precipitate on warming
"	3MP + F-11	Yellow-orange
"	MTHF	" "
Isoquinoline	MTHF	Blue
N-2-cycanoethylcyclohexyl- amine	Freon	Faint-yellow*
N-2-hydroxyethylcyclohexyl- amine	Freon	Yellow*
	3MP + F-11	Colorless
	Freon	Yellow*
Quinoline	3MP + F-11	Yellow*
	MTHF	Pink
Tetraphenylpyrrole	Freon	Yellow green (λ_{\max} 350, 420, 480)
Picolylamine	MTHF	sl-yellow
Pyrimidine	MTHF	Yellow-green
Triazole (1, 2, 4)	Freon	Yellow
	3MP + F-11	Colorless
	MTHF	Colorless
Triphenylimidazole	MTHF	Yellow
	3MP + F-11	Colorless

*(yellow color had a different hue from Freon 114B2 color and did not yield a reddish brown color on warming).

TABLE 7. PPP Calculation on Pyrrole, Pyrrole Radical Cation, and Pyrrole Radical Anion

Parameter values optimized for pyrrole (eV)

H_{NN} : -55.966 H_{22}, H_{55} : -38.749 H_{33}, H_{44} : -37.990
 H_{CN} : -1.7 H_{CC} (neighbor) : -2.759 H_{CC} (next neighbor) : -1.905
 (NN/NN) : 16.8 (CC/CC) : 10.4 $(II/33), (II/44)$: 6.065
 $(II/22), (II/55)$: 8.458 $(22/33), (44/55)$: 7.53
 $(22/44), (33/55)$: 5.751 $(33/44)$: 7.388 $(22/55)$: 5.754

Calculated and Experimental Transition Energies

<u>Species</u>	<u>Type Transition</u>	<u>Calculated (eV)</u>	<u>Experimental (eV)</u>
Pyrrole	S-S	5.62 (1B_1)	5.88
		7.19 (1A_1)	6.77
	S-T	4.19 (3B_1)	4.35
Pyrrole Radical Cation	D-D	1.16 (2A)	1.5
		3.78 (2A)	4.1 (?)
Pyrrole Radical Anion	D-D	1.83 (2A) 4.26 (2A)	

TABLE 8. PPP Calculation on Pyridine, Pyridine Radical Cation, and Pyridine Radical Anion

Parameter values (eV)

H_{NN} : -44.762 H₂₂, H₆₆ : -41.594 H₃₃, H₅₅ : -42.401

H₄₄ : -42.401 H_{CN} : -2.62 H_{CC} : -2.29

(NN/NN) : 14.485 (CC/CC) : 10.136 (II/33), (II/55) : 5.61

(II/44) : 3.467 (55/66), (44/55), (33/44), (22/33) : 7.514

(33/66) : (22/55) : 4.96 (44/66), (33/55), (22/66), (22/44) : 5.547

Calculated and Experimental Transition Energies

Species	Type Transition	Calculated (eV)		Experimental (eV)
		Hush et. al.	Present work	
Pyridine	S-S	5.01	5.16	4.94
		5.69	5.74	6.26
	S-T	7.39	7.20	7.07
		4.03	3.62	3.68
Pyridine Radical Cation	D-D		1.16 (² A)	3.3
			3.16 (² A)	
			3.83 (² B)	
Pyridine Radical Anion	D-D	2.66	2.58 (² B)	3.7
			4.02 (² A)	
		5.26	4.17 (² A)	5.08
		5.03	5.16 (² C)	

TABLE 9. PPP Calculation on Pyrimidine, Pyrimidine Radical Cation, and Pyrimidine Radical Anion

Parameter values (eV)

H_{NN} : -51.319 H_{22} : -42.300

H_{44} , H_{66} : -42.142 H_{55} : -41.904

H_{CN} : -2.620 H_{CC} : -2.290

(NN/NN) : 14.485 (CC/CC) : 10.136

(11/22), (22/33), (33/44), (11/66) : 7.777

(11/33) : 10.605 (11/44), (33/66) : 5.630

(22/44), (22/66), (44/66) : 4.965 (11/55), (33/55) : 4.995

(22/55) : 5.560 (44/55), (55/66) : 7.549

Calculated and Experimental Transition Energies

<u>Species</u>	<u>Type Transition</u>	<u>Calculated (eV)</u>		<u>Experimental (eV)</u>
		<u>Hush et. al.</u>	<u>Present work</u>	
Pyrimidine	S-S	5.28	5.69	5.08
Pyrimidine Radical Cation	D-D		2.14 (² A) 4.69(² B)	
Pyrimidine Radical Anion	D-D	2.86 5.09 5.47	4.17 (² A) 4.52 (² C)	3.75 4.97

TABLE 10. PPP Calculation on Cyclopentadiene

Parameter values (eV)

$H_{11}, H_{44} : -29.975 \quad H_{22} : -32.186$

H_{ij} (neighbors) : -2.29

(CC/CC) : 11.13 (11/22), (22/33), (33/44) : 7.649

(11/33) : (22/44) : 5.727 (11/44) : 5.439

Calculated and Experimental Lowest Transition Energies

<u>Species</u>	<u>Type Transition</u>	<u>Calculated energy (eV)</u>	<u>Experimental Energy (eV)</u>
Cyclopentadiene	S-S	4.39 (1B_1)	4.8
	S-T	2.18 (3B_1)	3.1

TABLE 11.

Cyclopentadiene Integrals Slater Exponent 1.0

Integral	<u>Atom Pair</u>				
	ab	ac	ad	bc	
(i/j)	.5634093	.2319934	.1936038	.5339315	
(ii/jj)	.2848168	.2010504	.1901081	.2776542	
(i/T/j)	.1614353	.03021277	.02088053	.14612400	
(ii V_j^{ion})	SCF	.3330835	.2103058	.1976791	.3196969
	Slat.	.3235641	.2086678	.1963364	.3114825
(ij V_j^{ion})	SCF	.2734945	.08301713	.0661704	.2529374
	Slat.	.2600742	.08033911	.0641756	.2408955
(ij/ij)	.1113775	.0158486	.01149512	.09964697	

TABLE I2. Cyclopentadiene Integrals Slater Exponent 1.2

Integral	ab	ac	Atom Pair	
			ad	bc
(i/j)	.45208814	.13944601	.11013530	.42048853
(ii/jj)	.30918567	.20803517	.19591333	.29982907
(ij/ij)	.083647283	.0069095417	.0042092304	.071626458
(i/T/j)	.15467827	.014478473	.0078541393	.13525986
(iV ^{ion} _j) SCF	.35405901	.21469056	.20131955	.33777629
Slat.	.34228372	.21293989	.19989514	.32766310
(ij V ^{ion} _j) SCF	.25937323	.055803438	.04181888	.23419474
	.24373324	.05357447	.04025845	.22047924

TABLE 13. Cyclopentadiene Integrals

Slater Exponent 1.4

Integral	ab	ac	ad	bc
(i/j)	.35415127	.080605853	.060131098	.32286353
(ii/jj)	.32655264	.21252835	.19965604	.31536321
(ij/ij)	.057916581	.0025536092	.0013841953	.047561839
(i/T/j)	.13372039	.0036124477	.000068387338	.11235618
(ii v^{ion_j}) ^{SCF}	.36716012	.21728359	.20349323	.34880286
Slat.	.35357503	.21547002	.20201994	.33727687
(ij v^{ion_j}) ^{SCF}	.23238287	.035192265	.02477383	.20472197
Slat.	.21623010	.03355378	.02369576	.19088299

TABLE 14. Cyclopentadiene Integrals

Slater Exponent 1.5

Integral	ab	ac	ad	bc
(i/j)	.27175342	.045132978	.031755593	.24258508
(ii/jj)	.33899306	.21562686	.20224297	.32636192
(ij/ij)	.037691626	.00086964908	-.00041842635	.029629831
(i/T/j)	.10554654	-.0022078827	-.0033196588	.084520331
(ii v^{ion_j}) ^{SCF}	.37528027	.21894746	.20490010	.35552581
Slat.	.36034262	.21709539	.20339433	.34297371
(ij v^{ion_j}) ^{SCF}	.19905056	.02112947	.01396498	.17102484
Slat.	.18372050	.02002613	.01328279	.15819802

TABLE 15. Cyclopentadiene Integrals

Slater Exponent 1.8

Integral	ab	ac	ad	bc	
(i/j)	.20482366	.024612487	.016316314	.1788885	
(ii/jj)	.34806234	.21787283	.20411631	.33433186	
(ij/ij)	.023305323	.00027725079	.00011819947	.017512512	
(i/T/j)	.076047551	-.0044000566	-.0040289018	.057213778	
(ii V^{ion}_j)	SCF	.38034371	.22008523	.20586691	.35968552
	Slat.	.36440120	.21820729	.20433776	.34639035
(ij V^{ion}_j)	SCF	.16441334	.01220078	.00756836	.13773877
	Slat.	.15074184	.01150453	.00716391	.12657082

TABLE 16. Cyclopentadiene Integrals

Slater Exponent 2.0

Integral	ab	ac	ad	bc	
(i/j)	.15198304	.013127231	.0081929209	.12978918	
(ii/jj)	.35484170	.21955689	.20551644	.34027938	
(ij/ij)	.013802622	.000083711490	.000031581069	.0099032873	
(i/T/j)	.049211835	-.0045380436	-.0034970947	.033738883	
(ii V^{ion}_j)	SCF	.3835499	.22090088	.20656137	.36232739
	Slat.	.36686173	.21900425	.20501453	.34848960
(ij V^{ion}_j)	SCF	.13179862	.00682530	.00397288	.10764089
	Slat.	.12017289	.00640732	.00374480	.09837164

REFERENCES

1. J. W. Dodd, F. J. Hopton and N. S. Hush, Proc. Chem. Soc., 61 (1962).
Ph.D. Thesis, F. J. Hopton, University of Bristol, 1962.
2. H. I. Josheck and L. I. Grossweiner, J. Am. Chem. Soc. 88, 3261 (1966).
3. O. Janssen and K. Funabashi, J. Chem. Phys. 46, 101 (1967) and references therein.
4. D. W. Skelly and W. H. Hamill, J. Chem. Phys. 43, 3497 (1965).
5. B. Brockelhurst, F. D. Russell and M. I. Savadatti, Trans. Faraday, Soc. 62, 1129 (1966).
6. W. A. Gibbon, G. Porter, and M. I. Savadatti, Nature 206, 1355 (1965).
7. R. Livingston, H. Zeldes, and E. H. Taylor, Disc. Faraday Soc., 19, 166 (1955).
8. N. A. Krohn, Chem. Tech. Division, Ann. Prog. Rept. May 31, 1966 ORNL 3945, P218-220.
9. J. K. Thomas, et. al., J. Phys. Chem. 70, 2409 (1966).
10. J. Calvert and J. Pitts, Photochemistry, p202, John Wiley (1966).
11. C. Reid, J. Chem. Phys. 21, 1806 (1953).
12. K. Kondo, M. R. Ronayne, J. P. Guarino and W. H. Hamill, J. Am. Chem. Soc. 86, 1297 (1964).
13. C. Helene, R. Santus and P. Douzou, Photochem. and Photobiol. 5, 127 (1966).
14. L. I. Grossweiner and W. A. Mulac, Rad. Res., 10, 515 (1959).
15. E. P. Bertin and W. H. Hamill, J. Am. Chem. Soc. 86, 1301 (1964).
16. J. P. Mittal and W. H. Hamill, J. Am. Chem. Soc. 89, 5749 (1967).
17. K. Watanabe, T. Nakagama and J. Mottl., U.S. Dept. Comm., NBS PB-158-317 (1959).
18. W. C. Meyer and A. C. Albrecht, J. Phys. Chem. 66, 1168 (1962).
19. S. K. Lower and M. A. El-Sayed, Chem. Rev. 66, 199 (1966).

20. R. G. Parr, 'The Quantum Theory of Molecular Electronic Structure', W. Benjamin, N.Y., (1963).
21. T. H. Dunning and V. McKoy, J. Chem. Phys. 47, 1735 (1967).
22. J. A. Pople, Proc. Phys. Soc. (London) A63, 81 (1955).
23. H. C. Longuet-Higgins and J. A. Pople, Proc. Phys. Soc. (London) A68, 591 (1955).
24. C. Zauli, J. Chem. Soc. 2204 (1960).
25. F. Campadelli and C. Zauli, Theor. Chim. Acta (Berlin) 4, 260 (1966).
26. G. E. Tauber, J. Chem. Phys. 29, 300 (1959). Computer program written by F. Bernardi, University of Bologna.
27. L. Savini, Thesis 1955, University of Bologna; A. Mangini and C. Zauli, J. Chem. Soc. 2210 (1960).
28. F. Bernardi and G. Pausco, Boll. Sci. Fac. Chim. Ind. Bologna 24, 155 (1966).
29. J. C. Slater, Rev. Mod. Phys. 25, 199 (1953).
30. P. Palmieri, University of Bologna, private communication.

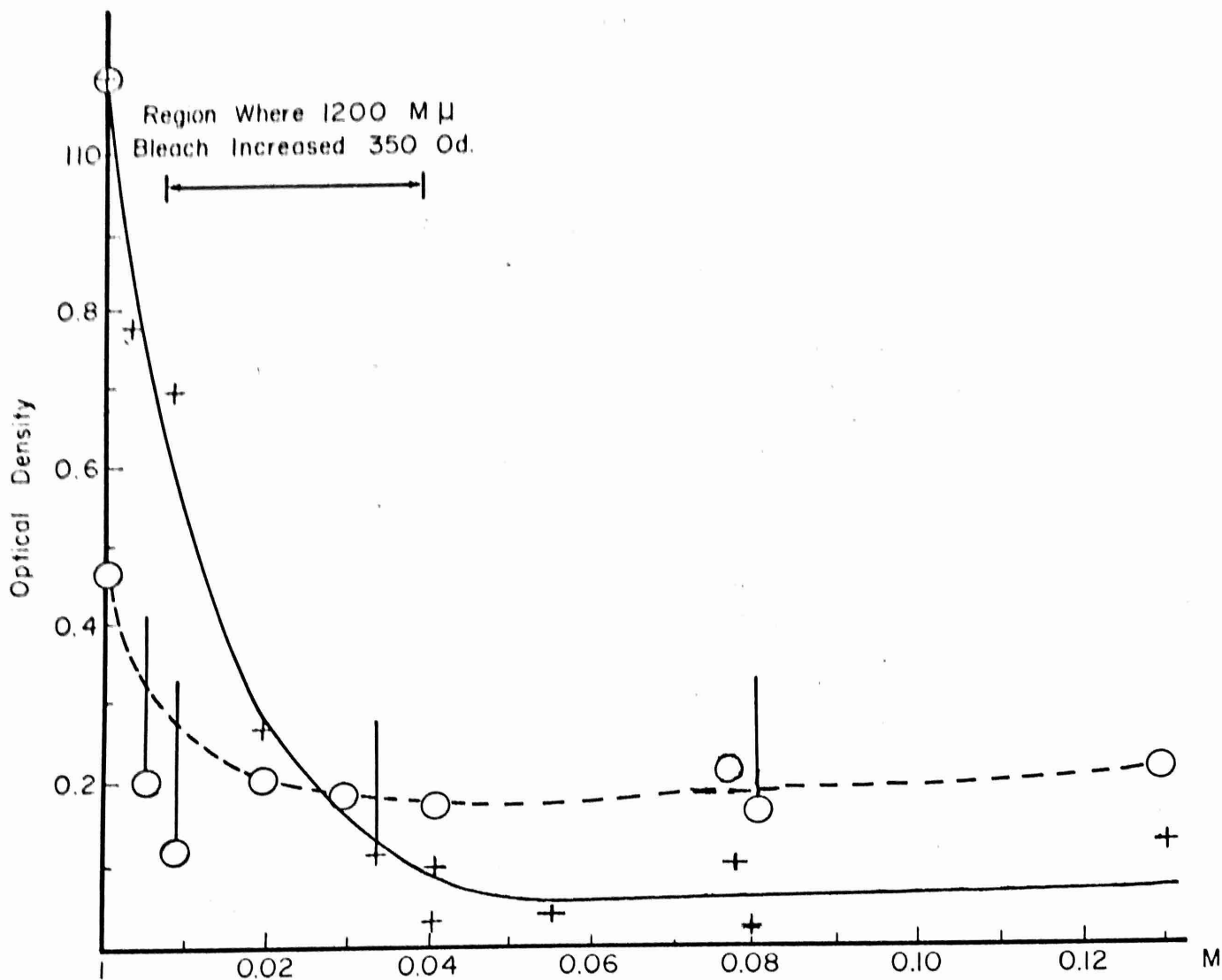


Figure 1 - Variation of Pyridine Concentration on the Yields of 1200 and 350 μ Absorption Bands in MTHF (dose = 1.9×10^{21})

— + — 1200 μ absorption
 --- o --- 350 μ absorption

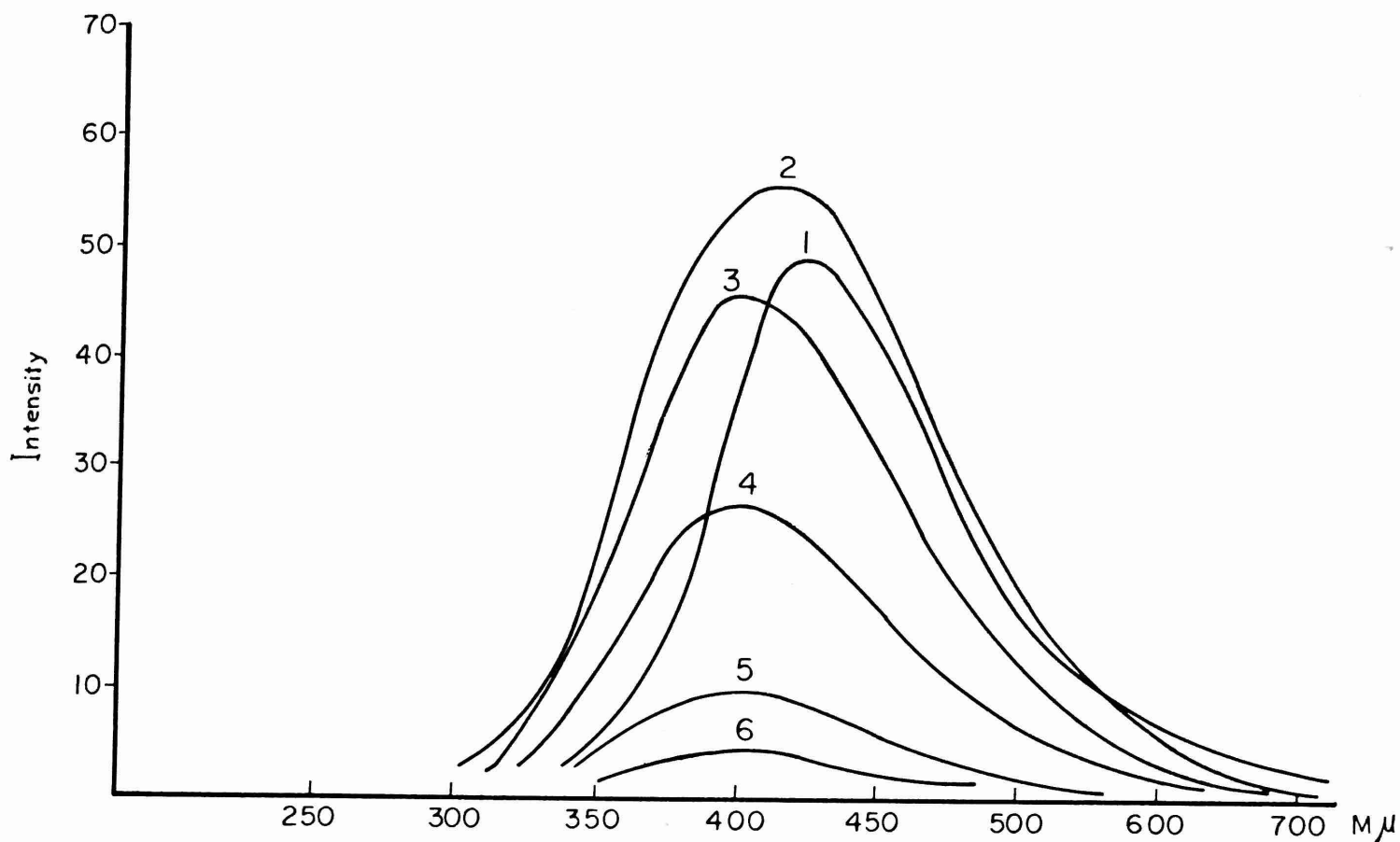


Figure 2 - "Warm-up" emission spectra of irradiated purified 3MeP dose on the order of 6×10^{21} ev/L.

Spectra No. 1 obtained within 30 seconds after
removal of liquid nitrogen (sensitivity
3X others)

No. 2 - 2.5 min. after liq. N₂ removal

No. 3 - 4.0 " " " " "

No. 4 - 6.0 " " " " "

No. 5 - 7.5 " " " " "

(Warm-up rate essentially linear for the first
4 minutes and is approx. 20%/min.)

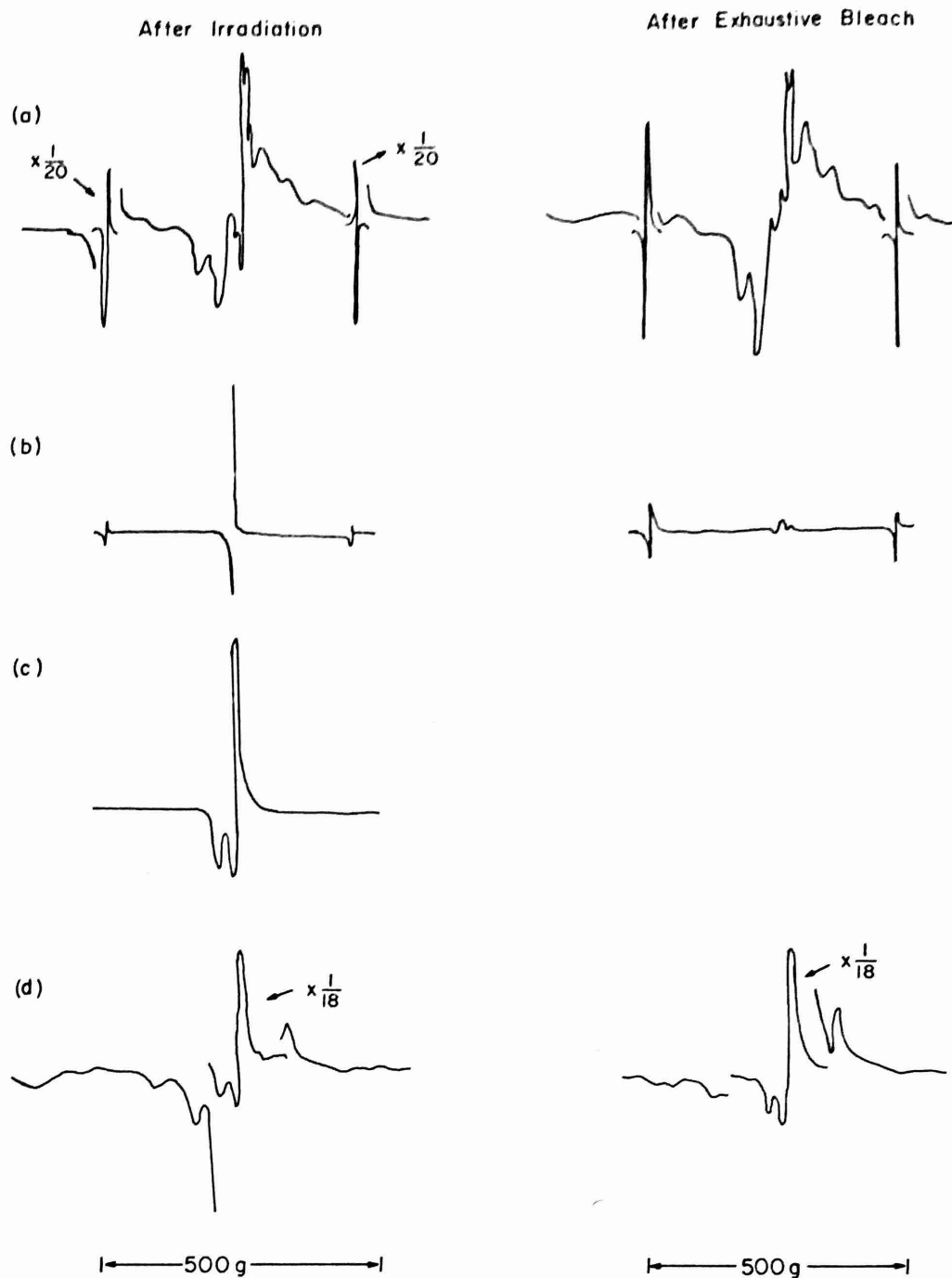


Figure 3 - ESR Spectra

- a) FM in silica tube
- b) Evacuated silica tube
- c) DM droplets prepared in air
- d) Degassed FM extruded from container under liquid nitrogen prior to ESR analysis

All doses of the order 2×10^{22} ev/L.

APPENDIX A

Journal of Physical Chemistry (in press)

SPECTROPHOTOMETRIC IDENTIFICATION OF GAMMA-RADIOLYTIC INTERMEDIATES
IN A NEW HALOGENIC GLASSY MATRIX*

A. Grimison and G. A. Simpson, Puerto Rico Nuclear Center*** and Chemistry
and Physics Departments, University of Puerto Rico, Río Piedras, P.R.

**Puerto Rico Nuclear Center is operated by the University of Puerto Rico
for the U.S. Atomic Energy Commission under Contract No. AT-(40-1)-1833.

ABSTRACT

The absorption spectra, dose dependence and character of the intermediates produced by gamma-radiolysis at 77°K of a 50-50 Vol. % mixture of Freon-11 (CCl_3F) and Freon-114B2 ($\text{CF}_2\text{Br CF}_2\text{Br}$) have been determined.

Color centers are formed at 330 $\text{m}\mu$ and 585 $\text{m}\mu$ which can be bleached by light of suitable wavelengths, and which are assigned to cationic species. The stabilization of other cationic intermediates by this matrix is demonstrated by the detection of intermediates of several heterocyclic additives. Identification of the following cations and their λ_{max} has been made: thiophene (830, 520 $\text{m}\mu$), pyrrole (800 $\text{m}\mu$), and pyridine (380 $\text{m}\mu$).

*Presented in part to the 1967, March Meeting of the American Physical Society, Bull. Am. Phys. Soc. 12, 423 (1967).

Hamill^{1,2} has discussed the usefulness of some halogenic matrices

-
- 1) T. Shida and W. H. Hamill, J. Chem. Phys. 44, 2369 (1966).
 - 2) T. Shida and W. H. Hamill, J. Chem. Phys. 44, 4372 (1966).
-

for isolation and spectrophotometric identification of gamma-radiolytic intermediates at 77°K. The matrices discussed, carbon tetrachloride and n-or s-butyl chloride, are either opaque or form cracked glasses at liquid nitrogen temperatures. Measurements of the absorption spectra of these matrices requires the use of short path lengths. Therefore, high concentration of reactant and high doses may be required to produce detectable spectra of radiolytic intermediates. These limitations can be avoided if a more transparent glassy matrix could be used, which retains the electron trapping and positive hole stabilization characteristics of the opaque solvents.^{1,2}

Sandorfy³ has discovered that a 50:50 vol. % mixture of Freon-11

-
- 3) C. Sandorfy, Can. Spectry, 10, 85 (1965).
-

(CCl₃F) and Freon-114B2 (CF₂BrCF₂Br) forms a stable, clear glass at 77°K suitable for spectroscopic studies. This matrix is transparent up to 3 cm. path length throughout the entire visible region to 2700 mμ, and is translucent for path lengths up to 20 cm.

The spectroscopic properties of the intermediates produced by radiolysis in this freon mixture (FM) have been determined. The ability of this matrix to stabilize the intermediates produced by radiolysis of

some dissolved heterocyclic compounds has also been investigated, and is reported here.

Experimental

The apparatus used to determine absorption spectra at 77°K with the Beckman DK1A spectrophotometer is shown in Figure 1. A brass dewar holder⁴

4) A scaled line diagram of the dewar, holder, and quartz cell is available in a Puerto Rico Nuclear Center publication, PRNC No. 88, 1966.

permits reproducible positioning of a rectangular quartz dewar in the sample beam of the spectrophotometer. The rectangular quartz dewar⁵ has

5) K. Funabashi, P.J. Herley, and M. Burton, J. Phys. Chem., 43, 3939 (1965).

been used previously for luminescence studies, but never described. It consists of General Electric Lamp Glass No. 204 square drawn quartz tubes attached concentrically by a ring seal and fused to quartz plates at the bottom. This design was preferred to that described by Farhataziz and Dyne⁶ for reasons of lower signal noise from nitrogen bubbles, and flexibi-

6) Farhataziz and P. J. Dyne, AECL, No. 2113, 1964.

lity in cell path length. Optical cells of 1 cm x 1 cm square Spectracil tubing, or up to 2.4 cm pyrex "Lollipop" cells could be used. Most of the spectrophotometric data reported here were obtained through the use of this apparatus in the Beckman DK1A. However, spectra of the individual components, which form opaque films, were usually determined in a H. S. Martin and Co. "cold finger" dewar, having an optical path of 1.6 mm,

using the Cary-14 spectrophotometer. All spectra were determined in times ranging from five minutes to two hours after irradiation.

E. I. Dupont or Matheson Freons were used after purification. Freon-11 was recrystallized twice at 77°K, retaining the liquor after half the material had solidified. Freon-114B2 was distilled twice, retaining a middle portion. The purification procedures were checked by VPC analysis. Methyltetrahydrofuran (Eastman Organic Chemicals, Co.) was passed over alumina under a nitrogen atmosphere, and then transferred under vacuum to a flask containing sodium-potassium alloy and stored until needed. N,N,N',N' tetramethyl-p-phenylenediamine (TMPD) was liberated from its dihydrochloride by addition of NaOH, then extracted with 3-methylpentane. The solution was evaporated and the solid sublimed and stored in the dark until the preparation of solutions. Resublimation was performed if discoloration occurred on standing. All other reagents were of the highest commercial purity and were distilled or sublimed prior to sample preparation.

Degassed solutions of the indicated molar concentration were prepared by conventional vacuum techniques using the required volume of FM which had been dried over molecular sieve (Type 3X) while under vacuum.

The dose rate was estimated using the Fricke dosimeter (the density of FM being $2.61 \pm .06$ g/cc at 77°K) in the optical cell in a dewar containing water.

Optical bleaching was performed with a 250 watt Sylvania Quartz-Iodine Lamp, using Corning color filters transmitting wavelengths greater than 460 m μ (CS NO. 3-71) or greater than 650 m μ (CS No. 2-64). Photolysis of TMPD was effected by 10 min. exposure of a sample (10^{-3} M) to an Osram HBO 500 lamp.

Results and Discussion

On gamma-irradiation a deep violet color is produced in the FM. The associated spectrum is shown in Figure 2, together with the effect of bleaching with wavelengths greater than $460 \text{ m}\mu$. The FM bands at 330 and $585 \text{ m}\mu$ are destroyed on bleaching. After bleaching there remains a broad absorption band having λ_{max} at $600 \text{ m}\mu$ which is unaffected by further bleaching. Absorption at wavelengths less than $270 \text{ m}\mu$ could not be determined due to the solvent cut-off, but the absorption between 270 and $300 \text{ m}\mu$ increases on bleaching. No other new absorption bands are produced. The variation of the optical density at $585 \text{ m}\mu$ with total dose, and with the extent of purification of the FM, is presented in Figure 3. This shows the $585 \text{ m}\mu$ absorption to be a linear function of the dose, and insensitive to further purification after two initial purification steps. The bands in irradiated FM are relatively stable, no obvious time dependence being observed for times up to 2 hrs. The efficiency of production of the $585 \text{ m}\mu$ band can be expressed as the product of the yield per 100 ev and the extinction coefficient. The value obtained from the slope of the curve in Figure 3 for purified FM and the dose rate is $G\epsilon = 4.5 \cdot 10^3 (\text{M cm})^{-1}$ (molecules/100 ev).

Bleaching the sample with light of wavelengths greater than $650 \text{ m}\mu$ and thus into the tail of $585 \text{ m}\mu$ band, produces only a decrease in the $585 \text{ m}\mu$ band. This indicates that the color centers at 330 and $585 \text{ m}\mu$ are associated with distinct entities, and that the $330 \text{ m}\mu$ band extends into the region 460μ to $650 \text{ m}\mu$. Variation of the FM composition results in a variation in both the relative intensities and positions of the 330 and $585 \text{ m}\mu$ bands. The absorption bands produced on gamma-radiolysis of the

separate components at 77°K were therefore determined, although aerated cells then had to be used, as distinct from the FM irradiations. For Freon-11, maxima are produced at 310 m μ and at 535 m μ , with a shoulder at 600 m μ . For Freon-114B2 a maximum is produced at 360 m μ . These absorption bands were also decreased on bleaching. These results show that the color centers in the FM are similar to, but not identical with, the color centers observed in the separate components.

Irradiation of a 0.15 V% solution of the FM in glassy MTHF at 77°K results in the trapped electron band of MTHF at 1200 m μ being decreased by 78% relative to the pure solvent. This indicates that the FM is very efficient in scavenging electrons. However, the bleachable bands cannot be assigned to species resulting from simple electron attachment to the FM. This was demonstrated by the photolysis of a solution of TMPD in the FM, as a source of low energy electrons. This photolysis produced the well-known absorption of the Wursters Blue cation, but no additional absorption resembling that observed in gamma-irradiated FM.

In order to test the possibility that the color centers observed in the FM are cationic in nature, an attempt was made to observe positive charge transfer on photostimulation. A solution of TMPD in the FM was gamma-irradiated so as to produce both FM color centers and TMPD cation absorption, but under conditions where a considerable concentration of TMPD neutral molecule remained. This sample was subsequently bleaching with light of wavelengths greater than 460 m μ , so that only the overlapping FM color centers and TMPD cation absorptions were excited. Since the TMPD cation⁶

6) W. C. Meyer and A. C. Albrecht, J. Phys. Chem. 66, 1168 (1962).

itself is inert to photostimulation, a photostimulated positive charge migration from the FM color center to TMPD neutral molecule should cause a decrease in the FM color center, and an increase in the TMPD cation absorption. The results are shown in Figure 4. These results are consistent with a decrease in the underlying FM absorption, and a concomitant increase in the TMPD cation absorption. Using the known relative optical densities of FM⁺ absorption at 585 and 630 m μ , and that of TMPD⁺ in the absence of any FM⁺ absorption, the spectrum in Fig. 6 can be resolved into its components. Thus, it is determined that FM⁺ has an optical density of 0.25 at 585 m μ before bleaching, and that TMPD⁺ has 1.16 and 1.57 od units at the same wavelengths before and after bleaching respectively. Under the conditions of the bleaching experiment both the 585 and the 330 m μ bands are completely removed in the absence of any additive. If it is assumed that only the positive species giving rise to the 585 m μ band react, and that all of those species are effective in causing an increase in the TMPD⁺ absorption, then a value of $\epsilon_{585} = 1.2 \times 10^4 / \text{M cm}$ is obtained using $\epsilon = 1.93 \times 10^4 (\text{M cm})^{-1}$ for TMPD⁺ at 585 m μ .⁶ This value may be high since the migration of cations associated with the 330 m μ band contributes to the TMPD⁺ increase, and since there is, presumably, some inefficiency in the charge transfer process. The value may be compared with that obtained from the oscillator strength equation,⁸ using the approximation $f = 4.32 \times 10^{-9} \epsilon_{\text{max}} \Delta \nu_{1/2}$

8) R. S. Mulliken, J. Chem. Phys. 7, 14 (1939).

The value of $\Delta \nu_{1/2} = 0.80 \times 10^4 \text{ cm}^{-1}$ is determined from the $\lambda_{1/2}$ values of 450 and 750 m μ . Assuming an $f = 1$, given the value of $\epsilon_{585} = 2.9 \times 10^4 / \text{M cm}$

which is approximately two times the earlier value, and provides a rough corroboration of the order of magnitude. Now use of the value of $\epsilon_{585} = 1.2 \times 10^4$ and the G value indicates that the efficiency of production of the 585 m μ FM species by radiation is greater than 0.4/100 eV.

The shifts observed in the λ_{\max} of the cation bands in the components and in FM suggests that the transitions associated with these cations are not restricted to isolated entities such as CCl_3F^+ and $\text{CF}_2\text{BrCF}_2\text{Br}^+$. The transitions may involve a participation of the solvent environment with these cations via electron exchange.

On the addition of small amounts ($\sim 10^{-2}\text{M}$) of various heterocyclic compounds to the FM and subsequent γ -irradiation, the yield of the solvent bands decreased, and new absorptions were produced. The results of these experiments are shown in Table 1. It is not probable that the solutes can compete effectively with the FM itself for electron trapping, so that negative intermediates of solutes are not expected in a halogen matrix. The results suggest that competition for positive charge formation in the matrix has occurred, and that new cationic intermediates⁹ are produced.

9) These experiments can not distinguish between a cation that is the direct result of the competition for positive charge formation, or an intermediate whose precursor is the primary cationic intermediate. For convenience the term cationic intermediates is used here.

The necessary and sufficient test for the existence of a cationic intermediate of an additive must be that not only does the additive depress the $(\text{FM})^+$ absorption, but also that on bleaching the $(\text{FM})^+$ absorption an increase in the absorption of the intermediates is produced.

Pyrrole, thiophene, and pyridine exhibit new absorption maxima as indicated, which increase on bleaching the solvent band. These absorptions are therefore assigned to cation intermediates of pyrrole, thiophene and pyridine. A preliminary Pariser-Parr-Pople SCF calculation,¹⁰ using

10) A. Grimison, unpublished results.

optimized parameters for the appropriate neutral molecule yielded transition energies of 1.04 and 3.43 eV for the pyrrole and pyridine radical cations respectively, against the above experimental values of 1.5 and 3.3 eV for the absorptions assigned to cationic species.

For the other additives an assignment cannot be made as readily. For imidazole, pyrimidine, pyridazine, and pyrazine the contribution of the intermediate is uncertain, due to overlap with the FM color centers. The solute intermediate absorptions decrease on bleaching, but the maxima can be obtained by suitable bleaching experiments, since the FM color centers disappear more readily. It is not certain whether imidazole gives an absorption maximum at 585 m μ or enhances the FM absorption at 585 m μ , since no residual absorption is obtained on bleaching. Furan also shows a decrease in the absorption of the intermediate on bleaching, but a new maximum is formed at 500 m μ . (The absorption of irradiated thiophene which increases on bleaching, also exhibits a new maximum at 530 m μ). A possible explanation of the decreases observed on bleaching intermediates from furan, imidazole, pyrimidine, pyrazine, and pyridazine is that these intermediates are photolytically unstable. The nature of these species is being further investigated.

The glassy FM matrix is recommended for use in isolating gamma-radiolytic intermediates because of its superior transmission properties, its ability to trap electrons irreversibly, to trap positive charges reversibly and to stabilize cationic intermediates.

Acknowledgement

The authors wish to thank Professor C. Sandorfy for suggesting this matrix, and Professor W. H. Hamill for much helpful discussion. This work was supported by a grant from the U.S.A.E.C. Division of Biology and Medicine.

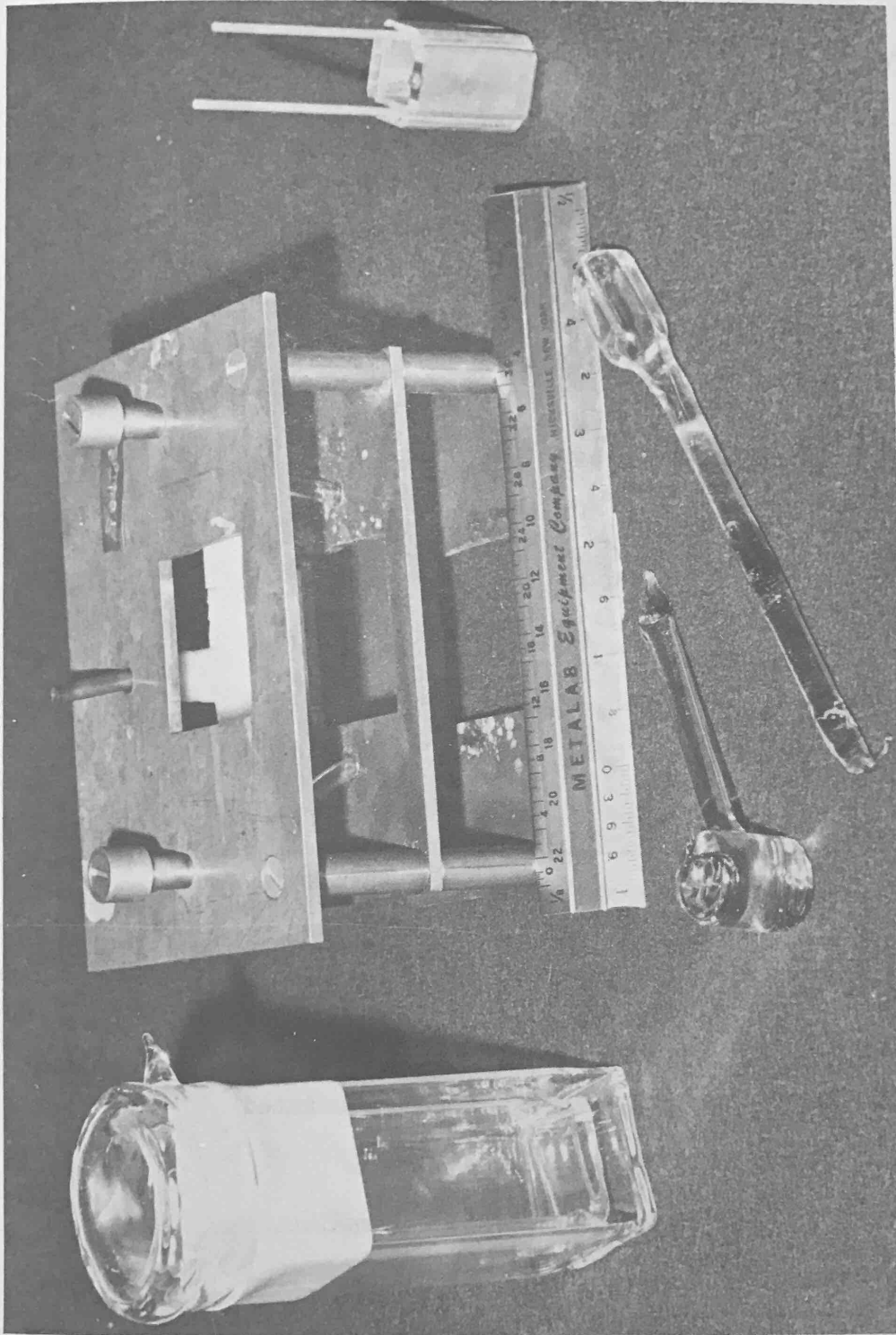


FIGURE 1. Optical equipment use with Beckman DK1a Spectrophotometer. Figure shows square quartz dewar, dewar holder, square quartz cells, cell holder, and pyrex "Lollipop" cell.

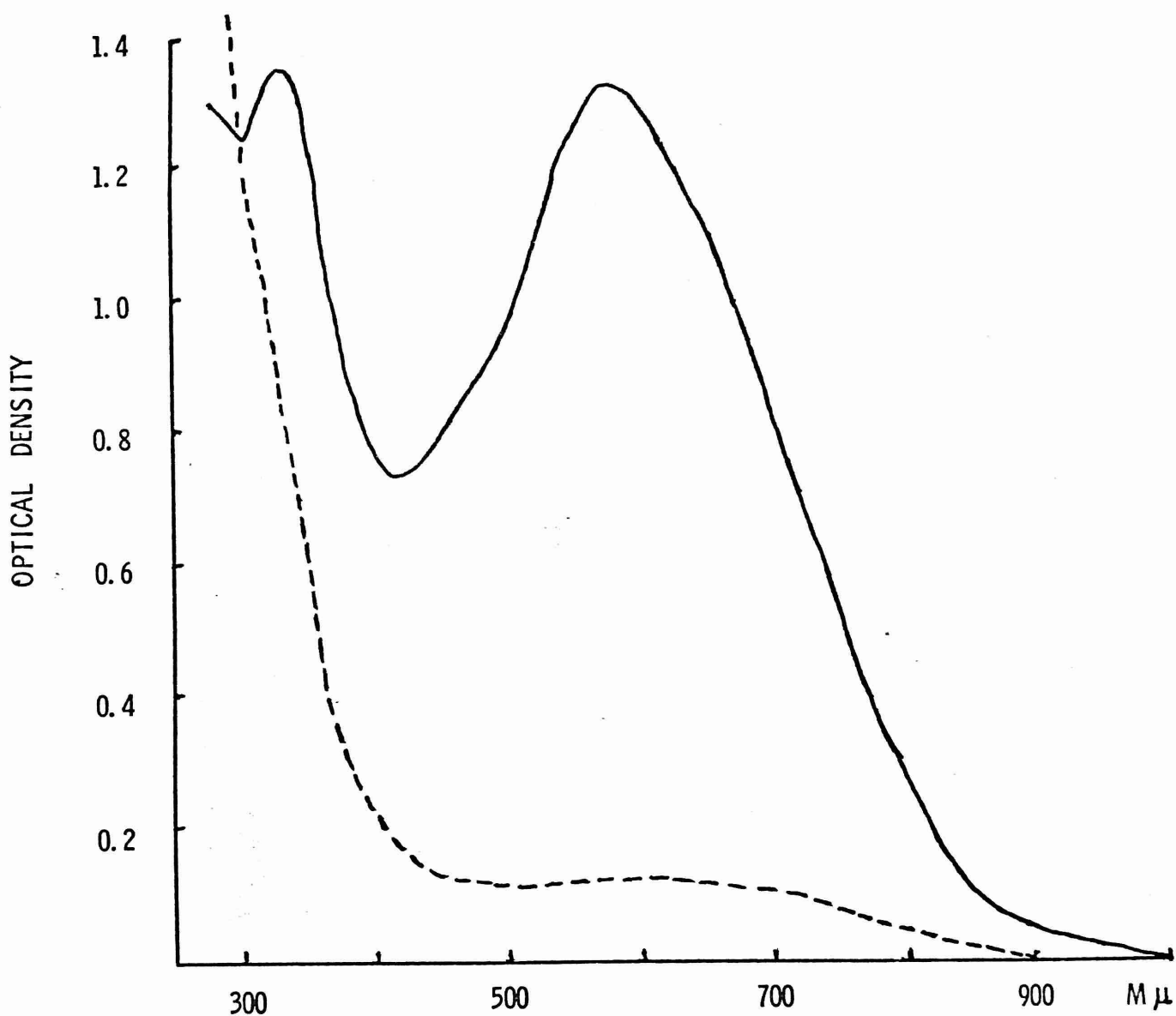


FIGURE 2. Absorption of doubly purified irradiated 50:50 V% mixture of Freon-11 and Freon-114B2 at 77°K; —after irradiation (1.6×10^{22} eV/l); -- after 20 min. photobleaching.

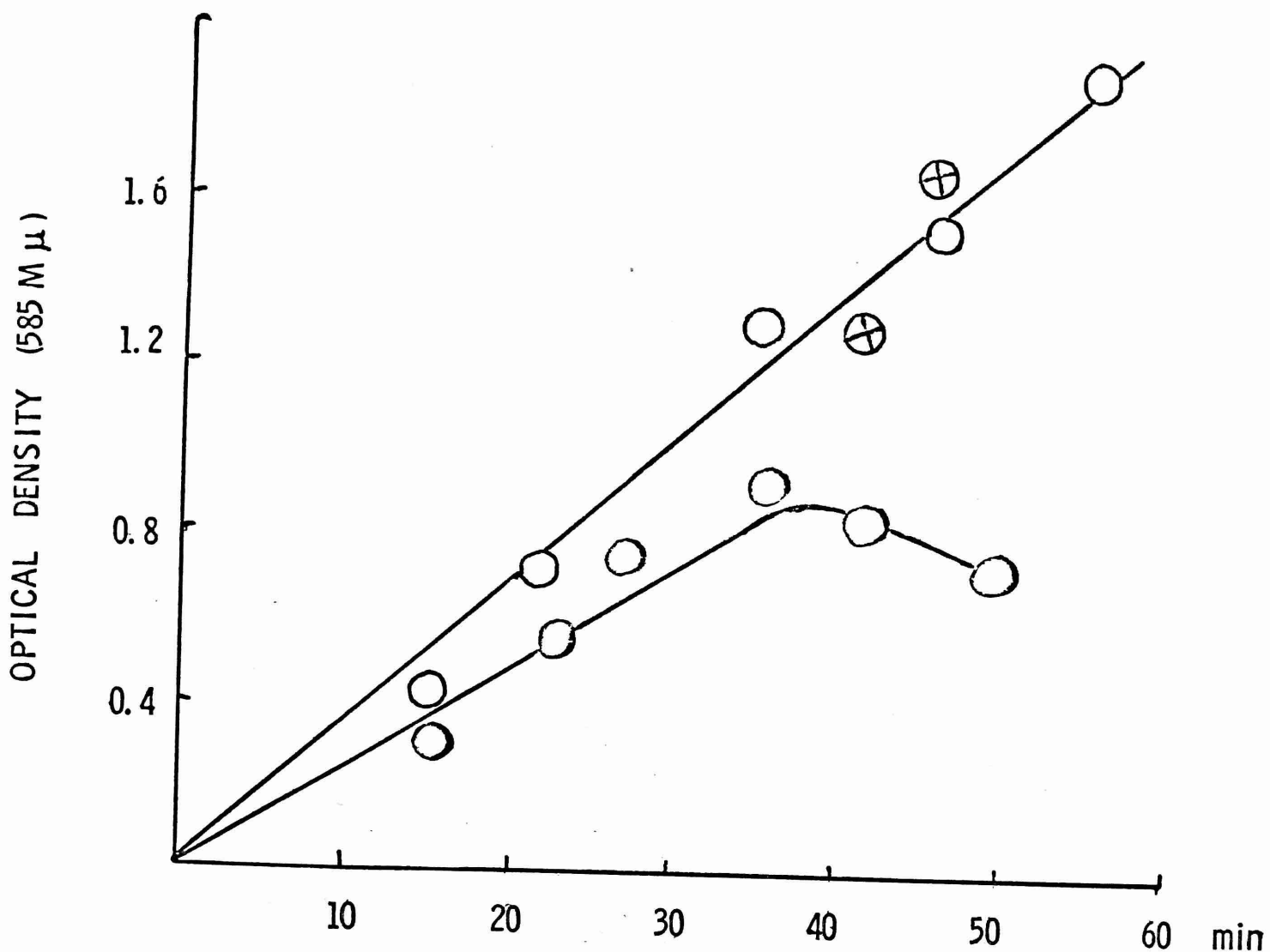


FIGURE 3. Optical density of irradiated 50:50 v% mixtures of Freon-11 and Freon-114B2 at 585 m μ vs. time of gamma-irradiation at 4.7×10^{20} ev/l min. and 77°K.

● - E.I. Dupont Co. reagents; ○ - doubly purified reagents (Freon-11 - recrystallization; Freon-114B2 - distillation); ⊕ - triply purified reagents.

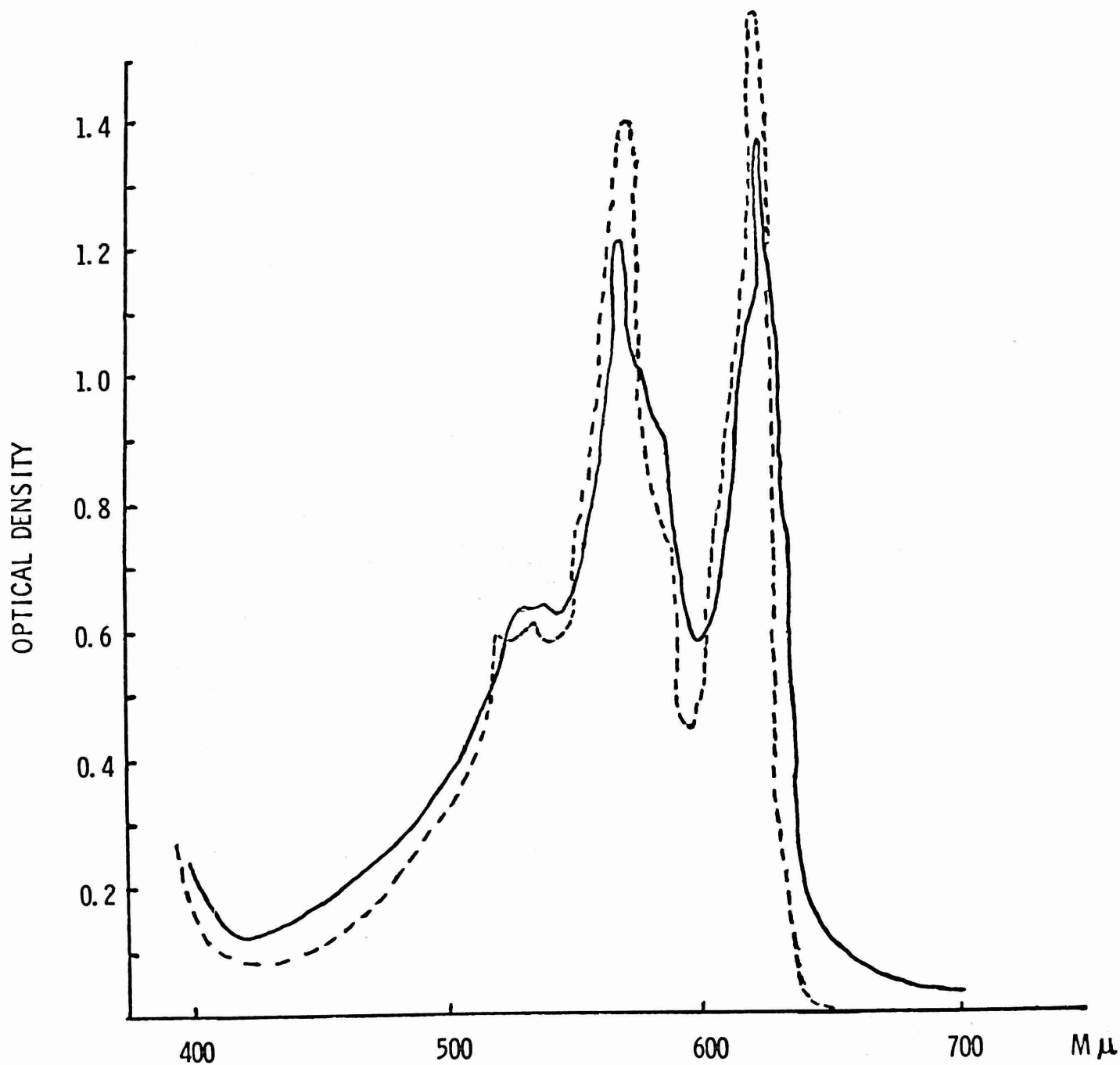


FIGURE 4. Absorption spectrum of irradiated
 N,N,N',N' tetramethyl-p-phenylene-
 diamine (1×10^{-2} M in FM at 77°K)
 (Dose rate = 4.7×10^{20} eV/1 min.).
 — After 10 min. irradiation.
 --- After 10 min. bleach ($\lambda > 460$ mμ).

TABLE 1

EFFECTS OF HETEROCYCLIC ADDITIVES ON γ -IRRADIATED FM AT 77°K

Solute	Conc. M	λ_{max} solute intermediate m μ	OD 585 m μ *	OD solute* at λ_{max}	Change in heterocyclic band on bleaching solvent band
None	--	--	1.00	--	--
Furan	4.6×10^{-2}	1000, 710	0.17	0.30, 1.00	decrease, form λ_{max} 500 m μ
Thiophene	4.2×10^{-2}	830, 320	0.11	0.14, 0.65	increase, form λ_{max} 530 m μ
Pyrrole	2.9×10^{-2} m/l	800	0.39	1.77	increase
Imidazole	Saturated	580	1.40		decrease
Pyridine	5.1×10^{-3}	380	0.72	1.60	increase
Pyrimidine	2.2×10^{-1}	650	0.32	0.45	decrease
Pyrazine	1.3×10^{-1}	650	0.23	0.52	decrease
Pyridazine	2.2×10^{-2}	475 sh, 380sh	0.29	0.43, 0.40	decrease

* 1.3×10^{22} ev/l. dose